Communications in Physics, Vol. 30, No. 1 (2020), pp. 49-59
DOI:10.15625/0868-3166/30/1/14752

INTEGRATED CROSS SECTIONS OF THE PHOTO-NEUTRON REACTIONS INDUCED ON ^{197}AU WITH 60 MeV BREMSSTRAHLUNG

NGUYEN VAN DO[a,b,†], NGUYEN THANH LUAN[f,b], NGUYEN THI XUAN[c],
PHAM DUC KHUE[d], KIM TIEN THANH[b], BUI VAN LOAT[e],
NGUYEN THI HIEN[f] AND GUINYUN KIM[f]

[a]*Institute of Theoretical and Applied Research, Duy Tan University, 1 Phung Chi Kien, Hanoi 100000, Vietnam*

[b]*Institute of Physics, Vietnam Academy of Science and Technology, 10 Dao Tan, Hanoi, Viet Nam*

[c]*Graduate School of Science and Technology, VAST, 18 Hoang Quoc Viet, Hanoi, Vietnam*

[d]*Institute for Nuclear Science and Technology, VINATOM, 179 Hoang Quoc Viet, Hanoi, Vietnam*

[e]*VNU University of Science,334 Nguyen Trai, Hanoi, Vietnam*

[f]*Department of Physics, Kyungpook National University, Daegu 702-701, Republic of Korea*

[†]*E-mail:* ngvando@iop.vast.ac.vn

Received 01 January 2020
Accepted for publication 10 February 2020
Published 28 February 2020

Abstract. *Seven photo-neutron reactions ^{197}Au(γ ,xn)$^{197-x}$Au (with x = 1 – 7) produced by the bremsstrahlung end-point energy of 60 MeV were identified. In this work, we focus on the measurement of integrated cross sections. Experiments were carried out based on the activation method in combination with off-line gamma-ray spectrometric technique. The integrated cross section of the investigated reactions were determined relative to that of the monitoring reaction ^{197}Au(γ, n)^{196}Au. To validate the experimental results, theoretical predictions were also made using the computer code TALYS 1.9. The current integrated cross-sections of the ^{197}Au(γ ,xn)$^{197-x}$Au reactions with 60 MeV bremsstrahlung end point energy are measured for the first time.*

Keywords: photo-neutron reaction, Activation, bremsstrahlung, integrated cross section, TALYS 1.9.

Classification numbers: 25.20.LJ.

I. INTRODUCTION

The investigation of nuclear reactions can gain important information that facilitates our understanding of nuclear properties and/or reaction mechanisms. Among different types of nuclear reactions, photonuclear reactions are becoming increasingly important in fusion reactors and accelerator-driven sub-critical systems (ADS) [1,2], where high energy photons can be created and then interact with materials, and finally cause photonuclear reactions. In addition, the study of photonuclear reactions can in many cases provide useful nuclear data that is required in a variety of applications [3–7].

The photonuclear reaction requires threshold energy. Generally, they can only occur at energies greater than about 8 MeV. Due to the lack of high energy photon sources, most of photonuclear reactions have been so far performed in the Giant Dipole Resonance (GDR) energy region. Within the GDR energy range, where the end-point energy of bremsstrahlung is less than about 30 MeV, the photoreaction mechanism can be fairly well explained in terms of the compound nuclear model. However, in recent years, photonuclear reactions have been increasingly studied at higher energies, beyond GDR region due to the fast development of high energy bremsstrahlung sources based on high energy electron linacs. Thanks to this, multi-channel photonuclear reactions can be opened, and studies of such nuclear reactions have received much attention [8–12].

In this work, we selected the ^{197}Au(γ ,xn)$^{197\text{-x}}$Au photo-neutron reactions caused by the bremsstrahlung with end-point energy of 60 MeV for studies. The main purpose of the study is to determine the integrated cross sections of these reactions. In the literature, very few similar studies have been found in this energy region. Besides, gold is one of the mono-isotopic elements, very easy to prepare and in many cases can be used as a standard reaction [13,14]. Studies of multi-particle reactions such as ^{197}Au(γ ,xn)$^{197\text{-x}}$Au can obtain information regarding channel effects [15,16] as well as nuclear data that can be used for both research and applications, especially in activation experiments [17,18]. To confirm the validation of the experimental results, we also made theoretical predictions with the TALYS 1.9 computer code [19]. The results obtained are discussed.

II. METHODOLOGY

Most of the photonuclear reactions are performed with continuous-energy bremsstrahlung photons. Therefore, the measure of the photonuclear reaction is usually expressed as the integrated cross section (σ_{int}), which can be obtained by integrating the energy dependent cross section $\sigma(E)$ from the threshold (E_{th}) to the maximum (E_{γ}max) bremsstrahlung energies:

$$\sigma_{int} = \int_{E_{th}}^{E_{\gamma\max}} \sigma(E)dE \tag{1}$$

In this experiment, the integrated cross section can be derived from the measured reaction yield based on the relationship:

$$Y = N_0 \int_{E_{th}}^{E_{\gamma\max}} \sigma(E)\phi(E)dE = (\lambda S_{\gamma})/(N_0\varepsilon_{\gamma}I_{\gamma}F) \tag{2}$$

where λ is the decay constant, S_γ is the photo-peak area of the indicated gamma-ray, N_0 is the number of the target nuclei, ε_γ is the detection efficiency, I_γ is the intensity of the measured gamma-ray, and factor F reflects activity related to irradiation, waiting and counting times, namely:

$$F = \left[(1-e^{-\lambda_i \tau})e^{-\lambda_i (T-\tau)}/(1-e^{-\lambda_i T})\right]\left[(1-e^{-\lambda_i t_{irr}})e^{-\lambda_i t_w}(1-e^{-\lambda_i t_m})\right] \quad (3)$$

where τ is the pulse width, T is the cycle period, $t_{\rm irr}$ is the irradiation time, t_w is the waiting time and t_m is the measurement time.

As shown in Eqs. (2) and (3), the yield of nuclear reactions can be determined through the activity of the residual nuclei, which, in turn, is determined from the photo-peak area of the selected gamma-ray. The integrated cross section can be derived from the reaction yield. By applying the relative method, the integrated cross section of the reaction being studied can be determined relative to that of the monitoring reaction. By taking into account the difference between threshold energies of photoreactions, the integrated cross section of the nuclear reaction investigated can be derived from the following expression [20]:

$$\sigma_{{\rm int},x}/\sigma_{{\rm int},m} = k\,(Y_x/Y_m\,) \quad (4)$$

where Y_x and Y_m represent the yields for the investigated and monitor reactions, $\sigma_{int,x}$ and $\sigma_{int,m}$ are the integrated cross sections for the investigated and monitor reactions, k is the flux correction factor corresponding to the threshold energies of the two nuclear reactions, (x) and (m). The value of the factor k can be achieved as follows:

$$k = \bar{\phi}_{W,m}/\bar{\phi}_{W,x} \quad (5)$$

where $\bar{\phi}_{w,x}$ and $\bar{\phi}_{w,m}$ are the weighted average bremsstrahlung fluxes and their values can be obtained by calculations:

$$\bar{\phi}_{W,i} = \int_{E_{th}}^{E_{\gamma max}} \sigma_i(E)\phi(E)dE \Big/ \int_{E_{th}}^{E_{\gamma max}} \sigma_i(E)dE \quad (6)$$

where i represents the index x or m. In order to obtain the weighted average flux value as expressed in Eq. (6), the energy dependent cross sections were calculated using the code TALYS 1.9 [19] and the bremsstrahlung spectrum was estimated using the MCNPX code [21].

It should also be noted that, after having the weighted average bremsstrahlung flux, the integrated cross section may also be presented as follows:

$$\sigma_{int,i} = \frac{Y_i}{\bar{\phi}_{W,i}} \quad (7)$$

In this work we have chosen the photo-neutron reaction ^{197}Au(γ, n)^{196}Au as monitor. The integrated cross-section of the monitoring reaction was obtained by fitting the data sets of cross-section available in the literature.

III. EXPERIMENT

III.1. Sample irradiation

A gold sample with a purity of 99.95% in the form of a 0.1 mm thick metal foil and a size of 15 mm x 15 mm was irradiated with the bremsstrahlung radiations at the electron linac of the Pohang Accelerator Laboratory (PAL), POSTECH, Korea. Details of the electron linac and the

bremsstrahlung production have been described elsewhere [22,23]. The bremsstrahlung radiations used in the present study were produced by bombarding the W target with the electron beam of 60 MeV and a beam current of 65 mA. The bremsstrahlung spectrum was simulated based on the experimental setup using computer code MCNPX [21] and shown in Fig. 1.

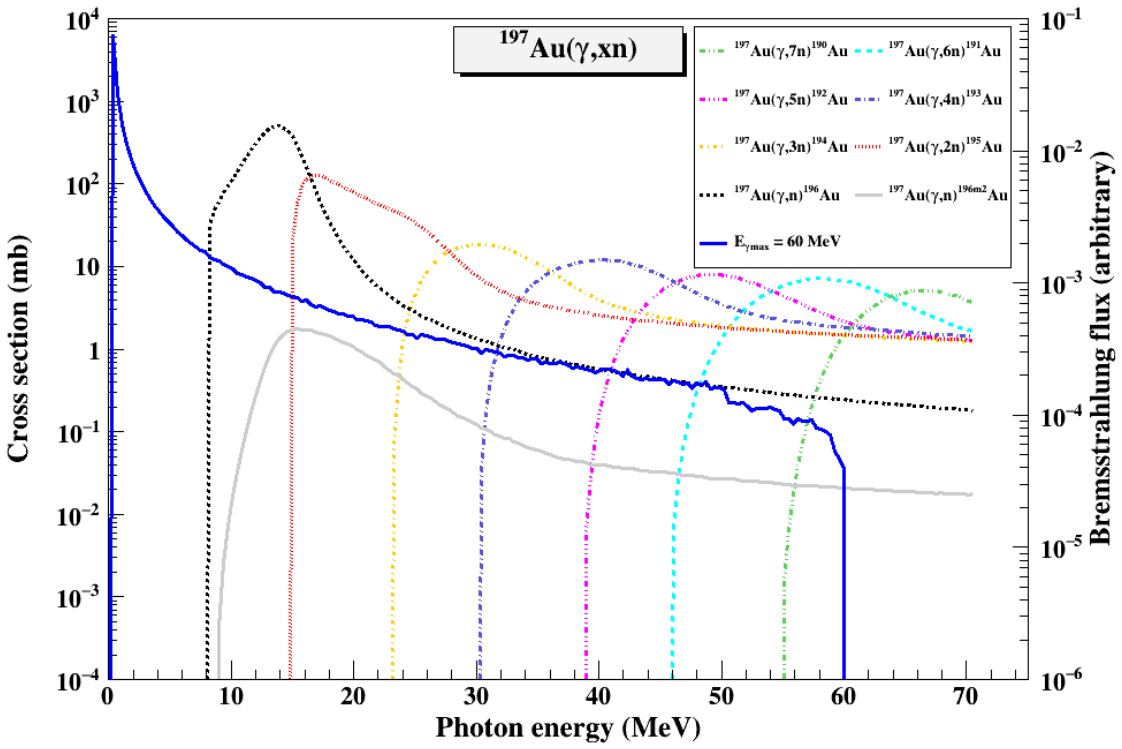

Fig. 1. Simulated bremsstrahlung spectrum generated from W target (with 0.1 mm thick, 100 mm × 100 mm size) bombarded with 60 MeV electron beam and theoretical cross sections of the ^{197}Au(γ, xn)$^{197\text{-}x}$Au reactions (with $x = 1$–7) calculated using the TALYS 1.9 code.

The cross section of photo-neutron reactions that can occur due to the interaction of 60 MeV bremsstrahlung end-point energy with the gold nucleus was also calculated with TALYS 1.9 [19]. Nowadays the code TALYS is widely used to predict and analyze nuclear reactions. This code simulates reactions that involve neutrons, gamma-rays, protons, deuterons, tritons, helium (^{3}He and ^{4}He) and alpha-particles with initial energy from 1 keV to 200 MeV and for target mass higher than 12. The calculations made in this article are based on theoretical analysis using optical model, compound nuclear mechanism, direct reaction and pre-equilibrium process, combined with databases and the necessary models for nuclear structure and reaction. The theoretically estimated cross sections for the ^{197}Au(γ ,xn)$^{197\text{-}x}$Au (with $x = 1 - 7$) nuclear reactions were also plotted in Fig. 1. The threshold energies are in the range from about 8 to 55 MeV. Details of the photo-neutron reactions caused by the interaction of bremsstrahlung with end-point energy of 60 MeV with gold nucleus are given in Table 1.

Table 1. Nuclear reactions ^{197}Au(γ, xn)$^{197-x}$Au and their main decay data [24].

Nuclear reaction	Threshold energy (MeV)	Half-life	Main γ-ray energy (keV)	γ-ray intensity (%)
^{197}Au(γ, n)^{196}Au	8.07	6.1669 d	333.03 355.73 426.10	22.9 87 6.6
^{197}Au(γ ,2n)^{195}Au	14.71	186.01 d	98.857	11.21
^{197}Au(γ ,3n)^{194}Au	23.08	38.02 h	293.55 328.46 645.15 948.31 1104.04 1175.35 1468.88	10.58 60.4 2.34 2.28 2.14 2.11 6.61
^{197}Au(γ, 4n)^{193}Au	30.46	17.65 h	112.515 173.52 186.17 255.57 268.22 439.04	2.2 2.8 9.7 6.5 3.8 1.85
^{197}Au(γ ,5n)^{192}Au	38.73	4.994 h	295.95 308.45 316.51 468.07 582.70 612.46 1706.63 1723.00	23 3.5 59 2.1 2.7 4.4 1.95 3.5
^{197}Au(γ ,6n)^{191}Au	45.73	3.18 h	277.86 283.90 413.73 586.44	6.4 5.9 3.3 15.0
^{197}Au(γ ,7n)^{190}Au	54.81	42.8 m	295.82 301.82 318.96 597.68	90 29.7 5.9 12.0

III.2. Activity measurement

The induced activities of residual nuclei were measured with a well calibrated HPGe gamma-ray detector (model ORTEC- GEM- 20180-p) connected to a PC-based multichannel analyzer. The energy resolution of the detector at the 1332.5-keV γ-ray of ^{60}Co is 1.8 keV and the detection efficiency is 20% relative to a $3'' \times 3''$ NaI(Tl) detector, respectively. The gamma-ray energy and photo-peak efficiency of the detector were calibrated using a set of the standard gamma-ray sources. In order to suppress the coincidence summing and pulse pile-up effects as well as keep the dead time less than about 5% each activated foil to be measured was placed at a distance of 10 cm from the surface of the HPGe detector.

The experiment focused on identifying reaction products and determining integrated cross sections for the nuclear reactions. The identification of reaction products is based on their half-life and gamma-ray energies. For long-lived isotopes, more gamma-ray spectra were taken at different waiting times to follow their decays as well as identify the possible interference. In order to identify the reaction products and measure their respective activities, the measured gamma-ray spectra were analyzed by GammaVision computer code version 5.10 (EG& G, ORTEC), which could determine the energy and number of counts under the photo-peak of each gamma-ray. To obtain the activity, several gamma-rays were analyzed, if it is possible. The integrated cross-section for each reaction can be derived from the measured gamma-ray activity. With the aim of improving the accuracy of the experimental results, corrections for the gamma-ray interference and counting losses were made. Typical gamma spectra of the irradiated gold sample are shown in Fig. 2.

As shown in Table 1 and Fig. 2, the activity of residual nuclides ^{196}Au can be determined from the gamma-rays of 333.03 keV, 355.73 keV, and 426.10 keV, which are considered as interference-free. However, if the measurement begins soon after the end of irradiation (less than about 5 hours), the contribution from the gamma-ray of 334.07 keV (0.06%) of ^{194}Au to 333.03 keV should be taken into account. For simplicity, the measurements of ^{196}Au were started several days after the end of the irradiation.

The activity of residual nuclides ^{195}Au was measured based on the gamma-ray of 98.86 keV. It is interfered by very small peak 99.88 keV (0.14%) of ^{193}Au. Fortunately, the ^{193}Au is a multi-gamma emitter. Therefore, in practice, the photo-peak area of the 99.88 keV can be extrapolated from other peak of ^{193}Au based on the so-called peak-ratio method [25].

The activity of residual nuclides ^{194}Au was determined based on the gamma-ray of 328.46 keV (60.4%). This gamma-ray is interference free and has a relatively high intensity. Some other gamma-rays having energies lower than 1000 keV are interfered by those from other isotopes such as ^{193}Au, ^{194}Au and ^{190}Au. In addition, the ^{194}Au has some gamma-rays with energy higher than 1000 keV, but their intensity is lower than that of the gamma ray 328.46 keV.

The residual nuclides ^{193}Au emit a number of gamma-rays with their energies between 112.51 keV and 439.04 keV. Some of them, such as 112.515 keV, 173.52 keV and 255.57 keV appear to be interference free and can be used for the measurement. However, these gamma- rays lie on a fairly high spectral background. Therefore, the combination of both manual and computer program was used in spectral analysis. By using more than one gamma-ray, an average yield of ^{193}Au was obtained.

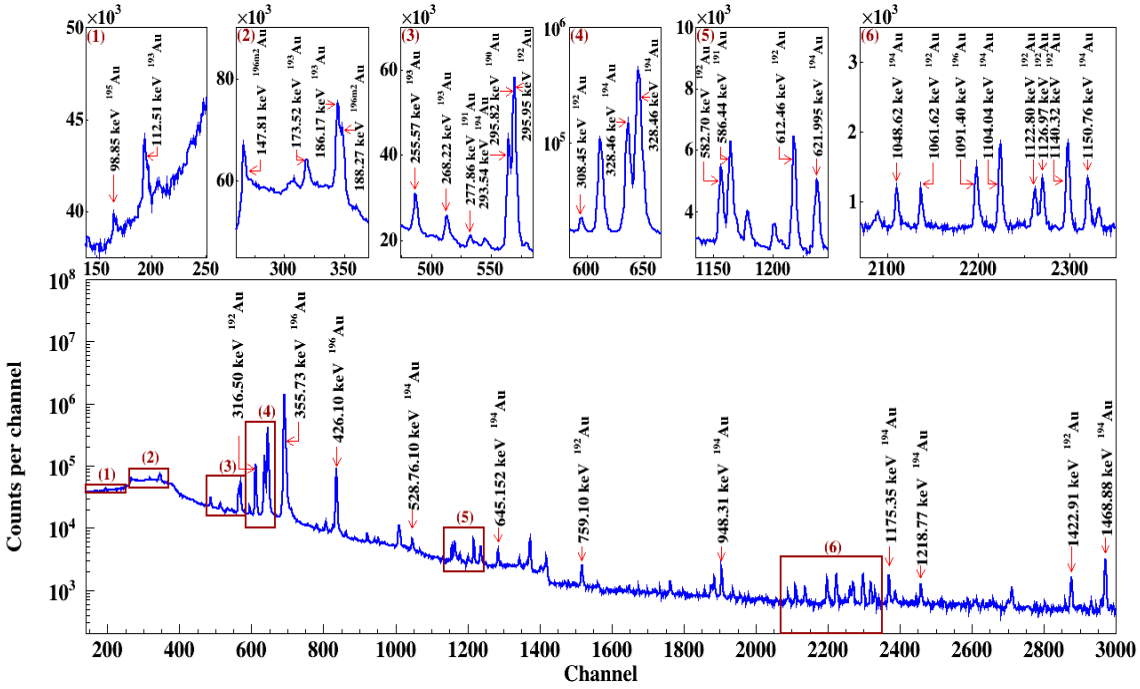

Fig. 2. Typical gamma-ray spectra of ^{197}Au(γ, xn) $^{197-x}$Aureaction products with the irradiation time of 3 hours, the waiting time of 50 minutes and the measurement time of 30 minutes.

The residual nuclides^{192}Au emit a number of gamma-rays and some of them such as 468.07 keV, 582.70 keV, 612.46 keV, 1706.63 keV and 1723.00 keV are interference-free. However, the intensity of these gamma-rays is relatively low. In addition, they are also lying on a high spectral background. In addition, although the gamma-ray of 316.51 keV has relatively high intensity, but it is overlapped by other gamma-rays such as 317.73 keV (0.23%) of ^{193}Au and 318.12 keV (0.21%) of ^{194}Au. Therefore, in this work, the activity measurement was performed based on the gamma-ray of 295.95 keV (23%). It should be noted that, if the measurement is made after a short waiting time, the contribution from the gamma-ray of 295.82 keV (90%) of ^{190}Au must be taken into account. However, after about 3 hours of waiting time, the gamma-ray of 295.95 keV is considered as interference-free because the half-life of ^{190}Au is relatively short (42.8 min).

The ^{191}Au residual nuclides emit a number of gamma-rays, but their intensities are relatively low. Although the 586.44 keV gamma ray has a relatively high intensity, 15% , it is not convenient to measure activity due to interference by gamma rays 589.19 keV (0.276%) from ^{194}Au and 588.58 keV (0.41%) from ^{192}Au. Fortunately, we have found some other gamma-rays with lower intensity, but they do not seem to be interfered. In this work, the 277.86 keV gamma-ray was used for the activity measurement.

The activity of the ^{190}Au radio nuclides was determined based on the gamma-rays of 295.82 keV (90%) and 301.82 keV (29.7%). In data processing, contribution from 295.95 keV of ^{192}Au to 295.82 keV was corrected. It should be noted that the activity of ^{190}Au isotope formed in gold foil irradiated with 60 MeV bremsstrahlung end-point energy is relatively low due to its threshold energy is relatively high.

III.3. Determination of integrated cross section

The integrated cross sections for the photo-neutron reactions ^{197}Au(γ ,xn)$^{197\text{-}x}$Au were determined relative to that of the monitor reaction. In this work, the nuclear reaction ^{197}Au(γ, n)^{196}Au was used as monitor. Fortunately, the integrated cross section data sets found in literature of the ^{197}Au(γ, n)^{196}Au reaction [26–31] covered the energy range from the threshold to 67.7 MeV. Plaisir *et al.* [26] provided the detail excitation function in energy range below 20 MeV. Based on that, the 11 values of integrated cross section for the ^{197}Au(γ, n)^{196}Au reaction can be obtained in the region from 10.1 to 20 MeV. Varlamov *et al.* [27] provided one integrated cross section data in the energy range from threshold to 17.94 MeV. Veyssiore *et al.* [28] provided 6 data in the energy range from threshold to 6 energy points in the range 8.35-19.77 MeV. Belov *et al.* [29] provided one data in the energy range from threshold to 25 MeV. Makarenkov *et al.* [30] and Ermakov *et al.* [31] each one provided one data in the energy range from threshold to 67.7 MeV. Thus, the integrated cross-section of the ^{197}Au(γ, n)^{196}Au reaction can be obtained by fitting the literature data. The fitting value obtained in the energy range from threshold to 60 MeV is 2399.98 $\pm$ 264.50 mb.MeV. The integrated cross-section for each nuclear reaction was obtained relative to this monitor value.

IV. RESULTS AND DISCUSSIONS

The present integrated cross sections for the nuclear reactions $^{197}\mathrm{Au}(\gamma,xn)^{197-x}\mathrm{Au}$ (with x = 1 – 7) using bremsstrahlung end-point energy of 60 MeV are given in Table 2. The experimental uncertainties were calculated by using the error propagation principle that contained measurement and systematic errors.

There are no reference data measured at the same energy for direct comparison with the present results. Therefore, the present data were validated by theoretical predictions using the computer code TALYS 1.9 [19].

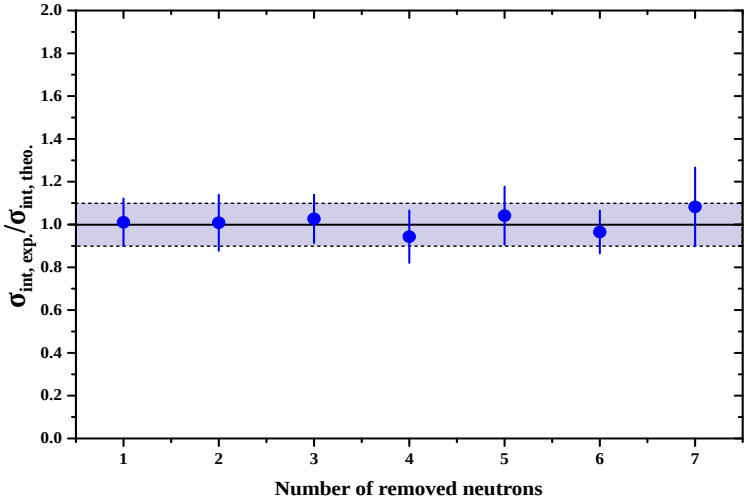

Fig. 3. Measured ($\sigma_{int,exp.}$) and calculated ($\sigma_{int,theo.}$) integrated cross-section ratios of ^{197}Au(γ, xn)$^{197\text{-}x}$Au reactions. The vertical axis represents the ratio, while the horizontal axis represents the number of removed neutrons from the gold nucleus (x = 1–7).

In calculation using the TALYS code, we have tested with 6 level density models [19]. The present experimental results are best suited to the predictions using the TALYS code with the level density model so-called constant temperature Fermi gas model (CTFGM) [19]. The calculated results using the CTFGM level density model are given in column 3 of Table 2. The deviations between the experimental and calculated data are less than 12% (see Fig. 3) except for the nuclear reaction ^{197}Au(γ, 7n)^{190}Au is about 17%.

In the literature we have also found some datasets of cross section for the ^{197}Au(γ, 2n)^{195}Au reaction [32–35]. For further comparison, we integrated these literature data sets from the threshold to 60 MeV. The obtained result is 902.39± 108.28 mb.MeV (see $**$ in column 5 of Table 2). It is well consistent with the present measured value of the ^{197}Au(γ ,2n)^{195}Au reaction, differ by about 5.5% . In column 5 of Table 2 we also give two data sets of integrated cross sections for the ^{197}Au(γ ,xn)$^{197\text{-x}}$Au reactions measured by Makarenkov *et al.* [30] and Ermakov *et al.* [31]. Although these reference data cannot be used to directly compare with current results, but they can show trends.

Table 2. Integrated cross sections for the ^{197}Au(γ ,xn)$^{197\text{-x}}$Au reactions induced by 60 MeV bremsstrahlung end-point energy.

Nuclear reaction	Experimental integrated cross section	Integrated cross section using TALYS-1.9 code	% Difference $*$	Literature data measured with $E_{\gamma,\max}$ = 67.7 MeV
^{197}Au(γ, n)^{196}Au	2399.98± 264.50	2375.74	1.02	2280± 200 [31] 2213± 210 [30]
^{197}Au(γ ,2n)^{195}Au	952.65± 123.84	944.88	0.80	730± 180 [31] 567± 100 [30] 902.39± 108.28$**$
^{197}Au(γ ,3n)^{194}Au	232.85± 25.61	226.89	2.62	240± 30 [31] 181± 30 [30]
^{197}Au(γ ,4n)193Au	144.23± 20.82	169.81	15.10	160± 20 [31] 162± 20 [30]
^{197}Au(γ ,5n)^{192}Au	100.16± 13.01	96.18	4.00	123± 10 [31] 123± 10 [30]
^{197}Au(γ ,6n)^{191}Au	54.91± 6.21	62.08	11.60	63± 15 [31] 67± 15 [30]
^{197}Au(γ ,7n)^{190}Au	5.41± 0.85	4.63	16.84	-

$*$ % Difference: the percentage difference = 100% x (1-this work/calculated value).

$**$ Integrated value obtained by integrating cross sections given in the literature [32–35].

V. CONCLUSION

We have identified seven photo-neutron reaction products (^{190}Au-^{196}Au) on gold target nucleus irradiated with 60 MeV bremsstrahlung end-point energy. The integrated cross sections of the ^{197}Au(γ,xn)$^{197-x}$Au reactions (with x = 1-7) were measured for the first time. It was found that up to 60 MeV bremsstrahlung end-point energy, the integrated cross-section of the ^{197}Au(γ,xn)$^{197-x}$Au reactions seems to decrease with increasing number of neutrons removed. The present results are validated by comparison with theoretical predictions using TALYS 1.9 computer code. The differences between experimental and theoretical results are within the error limits. This agreement tends to support the reliability of the present results. It is believed that the present data can be used for both scientific research and applications, especially in activation experiments.

ACKNOWLEDGEMENTS

The authors express their sincere thanks to the Pohang Accelerator Laboratory, POSTECH, Pohang, Korea for the valuable support to carry out this experiment. This research work is supported in part by the Vietnam National Foundation for Science and Technology Development (NAFOSTED) under Grant No. 103.04-2018.314.

REFERENCES

[1] R. Makwana, S. Mukherjee, Jian-Song Wang, Zhi-Qiang Chen, *Chinese Phys. C* **41** (4) (2017) 044105.
[2] I.S. Anderson, C. Andreani, J.M. Carpenter, G. Festa, G. Gorini,C.K. Loong, R. Senesi, *Physics Reports* **654** (2016) 1.
[3] A. P. Tonchev, J.F. Harmon, *Appl. Radiat. Isot.* **139** (2000) 873.
[4] J. Tickner, R. Bencardino, G. Roach, *Nucl. Instr. Meth*., *B* **268** (2010) 99.
[5] P. Mohr, S. Brieger, G. Wituci, M. Maetz, *Nucl. Instr. Meth*. *A* **580** (2007) 1201.
[6] M. Mantimin, F. Harmon, V. N. Starovoitova, *Appl. Radiat. Isot*., 102 (2015) 1.
[7] E. Vagena, S. Stoulos, *Nucl. Phys*., *A* **957** (2017) 259-273.
[8] A.K.M.L. Rahman, K. Kato, H. Arima, *J. Nucl. Sci. Tech*., **47** (2010) 618.
[9] A. P. Roberts, C. G. R. Geddes, N. Matlis, K. Nakamura, J. P. O'neil, B. H. Shaw, S. Stainke, J. V. Tilborg, W. P. Leemans, *Appl. Radiat. Isot.,* **96** (2015) 122.
[10] S.S. Belyshev, D.M. Filipescu, I. Gheoghe, B.S. Ishkhanov, V.V. Khankin, A.S. Kurilik, A.A. Kuznetsov,V.N. Orlin, N.N. Peskov, K.A. Stopani, O. Tesileanu, and V.V. Varlamov, *Eur. Phys. J.* **A 51** (2015) 67.
[11] N. V. Do, P. D. Khue, K. T. Thanh, N. T. Hien, G. N. Kim, K. W. Kim, S. G. Shin, Y. U. Kye, M. H. Cho, *Appl. Radiat. Isot.,* **128** (2017) 148.
[12] N. V. Do, K. T. Thanh, P. D. Khue, N. T. Hien , G. N. Kim, K. W. Kim, S. G. Shin, M. H. Cho, Y. U. Kye, *Radiat. Phys. Chem*., **149** (2018) 54.
[13] G. Steinhauser, S. Merz, F. Stadlbauer, *et al.*, *Gold Bull* **45** (2012) 17.
[14] N. V. Do, P. D. Khue, K. T. Thanh, N. T. Hien, G. N. Kim, K. W. Kim, S. G. Shin, Y. U. Kye, M. H. Cho, *Radiat. Phys. Chem.* **139** (2017) 109.
[15] N. K. Skobelev, Yu. E. Penionzhkevich, A. A. Kulko, N. A. Demekhina*a*, V. Kroh,A. Kugler, S. M. Lukyanov, J. Mrazek, Yu. G. Sobolev, V. A. Maslov,Yu. A. Muzychka, E. I. Voskoboynik, and A. S. Fomichev, *Physics of Particles and Nuclei Letters*, Vol. 10 (3) (2013) 248.
[16] H. Naik, G. N. Kim, K. W. Kim, M. Zaman, A. Goswami, M. W. Lee, S. C.Yang, Y. O. Lee, S. G. Shin and M. H. Cho, *Nucl. Phys. A* **948** (2016) 28.
[17] I. Semisalov, Ye. Skakun, V. Kasilov, V. Popov, *Problems of Atomic Science and Technology*, **N5** (93) (2014) 102.
[18] S. J. Alsufyani, L. R. Liegey, V. N. Starovoitova, *J. Radioanal. Nucl. Chem.* **302** (2014) 623.

[19] TALYS-1.9: A.J. Koning, S. Hilaire, S. Goriely, TALYS user manual, A nuclear reaction program, NRG-1755 ZG PETTEN (The Netherlands, 2017), available from https://tendl.web.psi.ch/tendl_2019/talys.html.
[20] N. V. Do, N.T. Xuan, N. T. Luan, N. T. Hien,G. N. Kim, IAEA- INDC(KOR)-006, Distr. NC. (2008) P. 42.
[21] J. S. Hendricks, W. M. Gregg, L. F. Michael, R. J. Michael, C. J. Russell, W. D. Joe, P. F.P. F. Joshua, B. P. Denise, S. W. Laurie, W. M. William, 2008. MCNPX 2.6.0 Extensions, LANL Report LA-UR-08-2216, Los Alamos, available from http://mcnpx.lanl.gov/.
[22] G. N. Kim, Y. S. Lee, V. Skoy, V. Kovalchuk, M. H. Cho, I. S. Ko, W. Namkung, D. W. Lee, H.D. Kim, S. K. Ko, S. H. Park, D. S. Kim, T. I. Ro, Y. G. Min, *J. Korean Phys. Soc*. **38** (2001) 14.
[23] G. N. Kim, H. Ahmed, R. Machrafi, D.C. Son, V. Skoy, Y. S. Lee, H. Kang, M. H. Cho, I. S. Ko, W. Namkung, *Korean Phys. Soc*. **43** (2003) 479.
[24] National Nuclear Data Center, Brookhaven National Laboratory, available from http://www.nndc.bnl.gov/nudat2/.
[25] N. V. Do, P. D. Khue, K. T. Thanh, N. T. Hien, B. V. Loat, S. C. Yang, K. S. Kim, G. N. Kim, T. Y. Song, S. G. Shin, M. H. Cho, Y. U. Kye, M. W. Lee, *Nucl. Instr. Meth. B* **342** (2015) 188.
[26] C. Plaisir, F. Hannachi, F. Gobet, M. Tarisien, M. M. Aleonard, V. Meot, G. Gosselin, P. Morel, and B. Morillon, *Eur. Phys. J. A* **48** (2012) 68.
[27] V. V. Varlamov, N. N. Peskov, D.V. Rudenko, M.E. Stepanov, INDC(CCP)-440 Series: Nuclear Constants 1-2 (2003) (Translated from Russian).
[28] A. Veyssiere, H. Beil, R. Bergere, P. Carlos and A. Lepretre, *Nuclear Physics A* **159** (1970) 561.
[29] A. G. Belov, Yu. P. Gangrskii, K. K. Gudima and P. Zuzaan, *Atomic Energy* **88-5** (2000) 408.
[30] I. V. Makarenkov, Kyaw Kyaw Htun, *Report in Moscow State Univ. Inst. of Nucl. Phys. Reports* 2007-2/823 (2007) (in Russian).
[31] A. N. Ermakov, B. S. Ishkhanov, I. M. Kapitonov, Kyaw Kyaw Htun, I. V. Makarenkov, V. N. Orlin and V. I. Shvedunov, *Physics of Atomic Nuclei* **71-3** (2008) 397.
[32] V. V. Varlamov, N. N. Peskov, D. V. Rudenko and M. E. Stepanov, *INDC(CCP)-440 Series: Nuclear Constants*, **1-2** (2003) (Translated from Russian)
[33] B. L. Berman, R.E. Pywell, S.S. Dietrich, M.N. Thompson, K.G. McNeill, and J.W. Jury, *Phys.Rev. C* **36-4** (1987) 1286.
[34] A. Veyssiere, H. Beil, R. Bergere, P. Carlos and A. Lepretre, *Nucl. Phys. A* **159** (1970) 561.
[35] S. C. Fultz, R. L. Bramblett, J. T. Caldwell, and N. A. Kerr, *Phys. Rev.* **127-4** (1962) 1273.